

POAR: Efficient Policy Optimization via Online Abstract State Representation Learning

Zhaorun Chen¹, Siqi Fan², Yuan Tan², Liang Gong^{3*},
Binhao Chen³, Te Sun³, David Filliat⁴, Natalia Díaz-Rodríguez⁴,
Chengliang Liu³

¹*Elmore Family School of Electrical and Computer Engineering,
Purdue University, West Lafayette, Indiana, USA.

²School of Information Science and Engineering, Lanzhou University,
Lanzhou, China.

³School of Mechanical Engineering, Shanghai Jiaotong University,
Shanghai, China.

⁴Flowers Team, ENSTA Paris, Institut Polytechnique de Paris &
INRIA, Paris, France.

*Corresponding author(s). E-mail(s): gongliang_mi@sjtu.edu.cn;

Abstract

While the rapid progress of deep learning fuels end-to-end reinforcement learning (RL), direct application, especially in high-dimensional space like robotic scenarios still suffers from low sample efficiency. Therefore *State Representation Learning* (SRL) is proposed to specifically learn to encode task-relevant features from complex sensory data into low-dimensional states. However, the pervasive implementation of SRL is usually conducted by a decoupling strategy in which the observation-state mapping is learned separately, which is prone to over-fit. To handle such problem, we summarize the state-of-the-art (SOTA) SRL sub-tasks in previous works and present a new algorithm called *Policy Optimization via Abstract Representation* which integrates SRL into the policy optimization phase. Firstly, We engage RL loss to assist in updating SRL model so that the states can evolve to meet the demand of RL and maintain a good physical interpretation. Secondly, we introduce a dynamic loss weighting mechanism so that both models can efficiently adapt to each other. Thirdly, we introduce a new SRL prior called *domain resemblance* to leverage expert demonstration to improve SRL interpretations. Finally, we provide a real-time access of state graph to monitor the course of learning. Experiments indicate that POAR significantly outperforms SOTA

RL algorithms and decoupling SRL strategies in terms of sample efficiency and final rewards. We empirically verify POAR to efficiently handle tasks in high dimensions and facilitate training real-life robots directly from scratch.

Keywords: state representation learning, reinforcement learning, robotics, learning from demonstration

1 Introduction

While learning for robotics control has benefited from various recent advances in reinforcement learning (RL) [1, 2], learning from demonstration (LfD) [3, 4] and safe control [5, 6], the curse of high dimensionality [7] and embodiment transferrability [8] are the major two challenges for broader robotics generalizations and robust applications. State representation learning (SRL) [9] has proven to be an effective approach to handle them. Contrastive methods [10–12] learn a lower-dimensional representation by training a model to distinguish between positive and negative examples. Predictive methods such as [13] learn latent-space transition model by explicitly predicting the future states; [14] map the high-dimensional raw observations into a compact space via reconstruction. Another line of works [15] incorporate representation learning objectives to address the embodiment gap. [16–18] learns transferable representations across embodiments and [19, 20] searches for shared action representations.

Most previous SRL implementations [14, 21–23] follow a decoupling strategy that consists of two stages: **learning state representations**, which builds a representative state space for the robotic environment from raw images, and then **learning a task-specific policy**. Extensive studies [13, 14] show that training via SRL exhibits better performance than direct end-to-end training for some RL algorithms, in terms of sample efficiency and final convergence. One paradigm to SRL is to incorporate optimizing objective functions with some robotic priors (e.g. reconstruction model that consists of an auto-encoder [24] and the environmental model where both state representation and the transition function is learned altogether [25]). In [23], the authors introduced some intrinsic priors specifically for robotic scenes. However, these approaches all separately feed samples to train the SRL model before RL. Since the SRL model does not update with the exploration collected by RL agent, the learned state estimator is prone to overfit. Besides, the actual performance of SRL can be only confirmed by a posterior RL training.

In this study, we propose Policy Optimization via Abstract Representation (POAR), which summarizes the SRL sub-learning tasks in previous works (e.g. forward [26], inverse [27], auto-reconstruction [28], reward [29] prediction tasks) and integrates SRL into the RL policy phase (e.g. proximal policy optimization (PPO) [1]) for online adaptive policy optimization. We design the algorithm to update SRL and RL models simultaneously, where the learned representation can evolve to meet the demand of reinforcement learning and maintain a good physical interpretation. Moreover, we can retrieve the learned abstract representation in real-time to monitor the course of training and diagnose the policy. Prior works often encounter difficulty in optimizing

RL and SRL goals together, since they are sensitive to hyperparameters (e.g. weight parameter of losses) and often lead either one to collapse[30]. In this work, we leverage a dynamic loss weighting strategy to guarantee convergence for online optimization of both goals.

In addition, to better accustom RL algorithms to 3D robotic control scenarios, we introduce a new SRL prior which leverages expert demonstration[3, 31]. Internalizing demonstration to diminish searching space can efficiently tackle the cold-start problem in which explorations are lengthy and expensive, especially during early training stages [32]. To do so, POAR employs a demonstration-based prior to optimize the maximum mean discrepancy (MMD) [33] loss to reduce the distribution similarity between learned states and expert trajectories, so that the represented states can capture expert’s behavioral modes.

Experimental assessment on 3 simulation environments demonstrate that under generalized conditions, POAR exhibits greater convergence rate and better final performance than PPO baselines[1] and decoupling strategies[14]. Our main contributions can summarize as:

1. We summarize the SRL sub-learning tasks in previous SOTA works and propose a generic RL framework for high-dimensional input, which integrates SRL and RL where both models can evolve together to adapt to each other to learn a better state representation and policy.
2. By combining external demonstration, the learned states distribution adapt to resemble the expert trajectory, which mitigates the cold-start dilemma.
3. We provide a real-time access to learned states to better monitor the SRL model and diagnose the current policy, which facilitates interpretability in deep RL.
4. Through increasing sample efficiency via various approaches, POAR makes it possible to directly deploy the algorithm and train on real robots in highly stochastic and interaction-expensive environments.

2 Preliminaries and Problem Statements

2.1 Reinforcement Learning (RL)

In RL terminology, an agent interacts with the target environment to maximize the accumulative rewards received from the environment. At each time step t , the agent selects an action a_t corresponding to the input representation of the environment’s state s_t . As a consequence of its action, the agent receives a scalar reward r_{t+1} and transits to the next state s_{t+1} . This process can be reformulated as an infinite-horizon Markov decision process (MDP), defined by the tuple $(\mathcal{S}, \mathcal{A}, P, r)$, where \mathcal{S} is a finite set of states, \mathcal{A} is a finite set of actions, and $P : \mathcal{S} \times \mathcal{A} \times \mathcal{S} \rightarrow [0, 1]$ is the transition probability distribution, $r : \mathcal{S} \rightarrow \mathbb{R}$ is the reward function. Let π denote a stochastic policy $\pi : \mathcal{S} \times \mathcal{A} \rightarrow [0, 1]$ that determines distribution of agent’s action at each given state. The goal is to find an optimal control policy π^* that maximizes the expected discounted reward $J(\pi) = \mathbb{E}_{s_0, a_0, \dots} [\sum_{t=0}^T \gamma^t r(s_t)]$, where $\gamma \in [0, 1]$ denotes the discount factor.

2.2 State Representation Learning (SRL)

SRL learns a function: $f : \mathcal{O} \rightarrow \mathcal{S}$ that maps observations in high-dimension to informative low-dimensional states. While deep RL algorithms have shown that it is possible to learn a feasible control policy from raw observations, SRL can take advantage of low-dimensional and informative representations, instead of raw images captured from camera to solve tasks more efficiently [34]. Since SRL is usually conducted in an unsupervised manner, it demands advanced priors of the tasks.

Two mainstream works prove to address SRL effectively, in which we comprehensively review in our former survey [29]. Contrastive learning methods [10–12, 35] leverage the insight that similar states are closer to each other while dissimilar ones are pushed farther apart, to learn a lower-dimensional representation in an unsupervised manner. On the other hand, predictive methods leverage latent-space dynamics modeling as an auxiliary task. [14, 24, 28] employ an auto-encoder to find a reduced set of features that encode necessary information to reconstruct the observations. Let ϕ be an encoder that encodes an observation o_t to a latent state s_t , and ψ a decoder to reconstruct the original observation from s_t . With θ being parameters of the functions, the optimization of encoder and decoder can be formulated as:

$$\begin{aligned} s_t &= \phi(o_t; \theta_\phi) \\ \hat{o}_t &= \psi(s_t; \theta_\psi) \end{aligned}$$

In the training process, by optimizing the loss function (1) iteratively, we can derive a state estimator that encodes essential information of input observations:

$$\mathcal{L}_{reconstruct} = \frac{1}{2} (\|\hat{o}_t - o_t\|_2^2 + \|\hat{o}_{t+1} - o_{t+1}\|_2^2) \quad (1)$$

[26] proposed to learn the environment dynamics via predicting future states coupled with reward prediction. However, such system dynamic models are highly non-linear and stochastic that often lead the learned latent space to collapse [13]. [27] employs a pair of networks for both forward and inverse prediction. These works learn the observation-to-state mapping as part of learning some other functions such as the transition of the environment $\hat{s}_{t+1} = f(s_t, a_t; \theta_{fwd})$, where $s_t = \phi(o_t)$. Thus, by minimizing $\mathcal{L}_{forward} = \|\hat{s}_{t+1} - s_{t+1}\|_2^2$ we can learn the encoder ϕ together with the transitional function f . This approach is addressed as the *forward model*, while *inverse model* and *reward model* [29] are similar in concept but predict respectively the action a_t that agent takes at t and reward r_{t+1} for next state using s_t and s_{t+1} . Similarly, [13] proposed a multi-step latent prediction task that enforce the long-term learned state representation. In robotics, to learn such state representation is rather intuitive, considering the physical priors we can benefit from. For example, robot operations are all deployed in real physical platform that could be considered as 2 or 3 dimension, while their intrinsic features are usually position, orientation, speed or acceleration. Authors in [23] thus introduce some *robotic priors* that only pertain to tasks involving robots in real-world function. Since manually designing priors are tedious, [36] proposed to automatically search for top-performing auxiliary loss functions for SRL.

In our former work [14], we notice that the performance can be significantly boosted by combining the above prediction sub-tasks altogether.

2.3 Combining SRL Sub-tasks

In this work, we study how to effectively combine the prediction priors to effectively learn informative representation. We can either use the whole state to apply these different priors, or split the states and apply objective functions to different parts of the state space. One motivation to apply the *srl split* model is that losses have different magnitudes and each prior have specialized functionality, optimization of all models on the same space often leads to collapse, leaving some features unlearned[14]. Fig. 1 demonstrates an example of SRL with split dimension. We use the whole state to reconstruct the observations yet split state space into three parts for forward, inverse and reward model. This can enforce components to specialize in encoding different featuring representations.

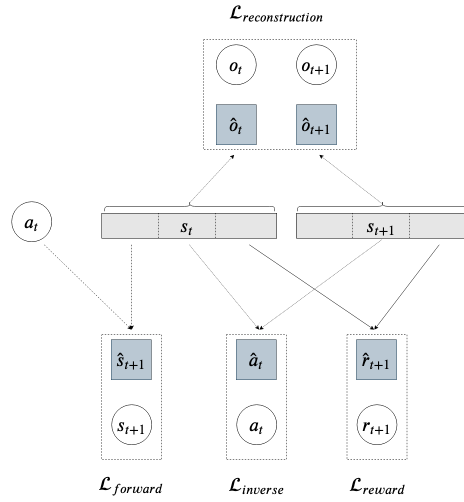


Fig. 1 SRL: The whole state is used to reconstruct the observations but state space is split into three part for forward, inverse and reward model.

By conducting SRL with above models, we can extract informative features into a lower dimension space. This process contributes on the one hand to accelerate the learning process so that it raises the possibility to train the RL agent directly on the robot. On the other hand, this low dimensionality offers an approach to interpret model extracted features, which facilitates the interpretability of deep RL methods.

3 Policy Optimization via Online Abstract Representation

Although SRL is confirmed to succeed in extracting some important features from high-dimensional sensory data, the state estimator derived from decoupling strategy usually deteriorates over the course of training[14, 34]. This is because the SRL model is only pre-trained with randomly sampled frames, whose parameters stay the same throughout the rest of the training, leading to over-fitting. Therefore, this work is inspired to combine the previous SOTA SRL sub-learning tasks and integrate these priors together with *domain resemblance prior* into the original PPO model, so as to update SRL adaptively throughout the training process. The design of POAR framework, *domain resemblance prior* is introduced in section 3.1, section 3.2. The general design of loss function and update strategy is explained in section 3.3.

3.1 POAR Optimization Framework

On the basis of the original framework of PPO, we integrate the SRL model and introduce a dynamic mechanism of loss weighting (discussed in section 3.3) to guarantee stability and convergence. We incorporate several effective priors in the model network, which takes advantage of the observation-action tuple (o_t, a_t) that PPO agent collects each batch to calculate loss based on predictions.

The proposed end-to-end state representation learning and reinforcement learning algorithm POAR is illustrated in Fig. 2. The detailed architecture and hyperparameters can be found in Appendix A1.

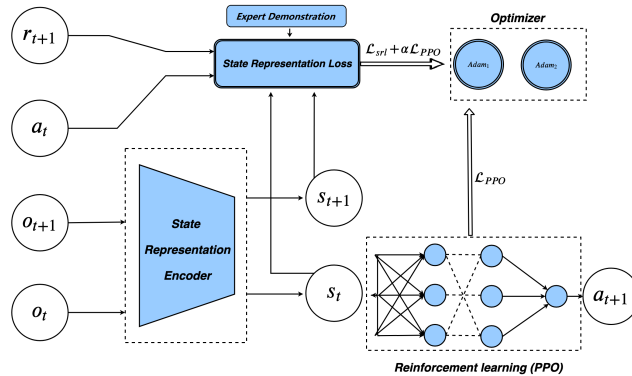


Fig. 2 The design of our proposed framework POAR: Policy Optimization with Online Abstract State Representation Learning, an end-to-end SRL-RL training pipeline.

In order to preserve the learned states to be representative for the physical meaning, we use two *Adam* optimizers (adaptive moment estimation) [37] that update separately the RL and SRL models. We add \mathcal{L}_{SRL} to assist in RL loss so that the states can evolve to meet the demand of reinforcement learning and maintain a good physical interpretability. By engaging RL loss to update SRL model, which pertains to learning

the encoder ϕ together with another function π^* , the state estimator is thus more robust and task-relevant.

This framework guarantees the timely update of SRL model, by which we obtain an effective and active representation of states. With the help of *domain resemblance prior*, our model can further boost the sample efficiency of RL training.

3.2 Domain Resemblance Prior

Simulation results show that directly using the task-relevant coordinates of robots as states to train RL agent can generally obtain better result than training from raw images[38, 39]. Therefore, we conceive the coordinate itself as a representational state, and seek to learn a mapping from raw image to ground-truth coordinates. To further guide the policy, we leverage expert demonstration as prior knowledge[4]. Thus we characterize portions of SRL states with robots’ coordinates in real-world (2D or 3D) and enforce the learned states resemble the distribution of expert trajectories. Considering that it’s not practical to provide accurate coordinate states for each camera frame when training a real-life robot, we apply *Maximum Mean Discrepancy* (MMD) [33] to measure the distribution deviation between sampled exploration and demonstration trajectories:

$$\mathcal{L}_{dr} = \left\| \frac{1}{n} \sum_{i=1}^n \Phi(\mathcal{D}_s) - \frac{1}{m} \sum_{j=1}^m \Phi(\mathcal{D}_d) \right\|_{\mathcal{H}}^2 \quad (2)$$

where $\Phi(\cdot)$ maps the original data to the regenerated *Hilbert* space [40]. By back-propagating the MMD loss, the learned states can effectively restore distribution of coordinates in the real work space, and also guide the RL agent to imitate expert’s behaviors[3]. We mainly use this prior to aid *forward* model on the same state portion to build a more structural understanding of the environment space. In conclusion, domain resemblance prior can facilitate the reconstruction of observations and increase interpretability of the learned state estimator.

3.3 Design of Loss Function and Update Strategy

With the presence of *Domain Resemblance* prior and some other useful priors like *forward*, *inverse* and *autoencoder*, the SRL model is promising to learn an efficient and task-relevant representation with strong physical interpretations. The loss function can be formulated as:

$$\begin{aligned} \mathcal{L}_{RL} &= \mathcal{L}_{PPO} && (\text{Optimizer1}) \\ \mathcal{L}_{SRL} &= \sum_{x \in \text{SRL Model}} w_x \times \mathcal{L}_x && (\text{Optimizer2}) \\ &= w_{iv} \mathcal{L}_{iv} + w_{fw} \mathcal{L}_{fw} + w_{rw} \mathcal{L}_{rw} + w_{ae} \mathcal{L}_{ae} + w_{dr} \mathcal{L}_{dr} \end{aligned}$$

where w_x denotes the weights attributed to each SRL sub-learning tasks.

Nevertheless, a direct optimization on two losses is prone to deteriorate the encoder. The overall model parameters can be back-propagated by both the SRL encoder and RL losses, while the latter are generally larger than that of SRL, which might lead

to the collapse (reduced to a point or strongly deformed) of states[29]. Therefore, we reduce scales of RL gradients on encoder part for *Optimizer 1*. Let denote θ as parameters, Θ_{SRL} , Θ_{RL} as the sets of parameters respectively concerning SRL model and RL model. If $\theta \in \Theta_{SRL} \cap \Theta_{RL}$, then:

$$Grad_{\text{Optimizer}_1}(\theta) = \alpha \times \frac{\partial \mathcal{L}_{RL}}{\partial \theta} \quad (3)$$

where α is a hyperparameter to balance the trade-off on optimization of PPO and SRL model on encoder part. Later in section 4.3 we present an ablation study on the best choices of α . We notice in our experiments that the SRL model generally converges long before the RL policy (the randomness of the policy at the early stage of RL contributes to the fully optimization of SRL models while exploring the environment). Once the SRL model is optimized, we seek to maintain its properties by applying a different learning rate decay strategy for two optimizers: the learning rate of PPO model lr_1 decays linearly to zero till the end while the learning rate of SRL model lr_2 exhibits an exponential decay slope that decreases much faster.

$$lr_1 = lr_0^1 \times r; \quad lr_2 = lr_0^2 \times \max(\exp(-\beta r), 0.001r); \quad (4)$$

where $r = 1 - \frac{n-1}{N}$, n is the current time steps and N denotes the total number of time steps. β denotes another hyperparameter to control the weight decay of SRL model’s learning rate. We elaborate in section 4 on the effectiveness of this dynamic weighting strategy on guaranteeing the convergence and optimality of the learned policy.

4 Experimental Results

To comprehensively assess the performance of POAR, we select 3 robotic environments: *MobileRobot* which consists of a racing car navigating to reach a target in 2D, *Omnirobot* which consists of a robot circling around the target in Mujoco[41] and a mechanical robot manipulator *Jaka*, as illustrated in Fig. 3. For the ease of operation, we perform experiments on a simulation platform *RobotDrlSim* [31] developed by our lab. Please check the github repository ¹ for the algorithm implementation and the simulator. The comparison results are 3-folded: (1) POAR is first compared to SOTA deep RL algorithms [1] to assess the necessity of an explicit SRL feature extraction model; (2) POAR is compared to decoupling SRL methods[14] to demonstrate the effectiveness of evolving SRL models online to adapt to RL policy; (3) We also compare the performance of splitting and combining SRL priors for a stationary state space.

4.1 Quantitative Analysis

The robot in *MobileRobot* aims to reach the yellow target with as few steps as possible, by which it receives a positive reward (+1), while receiving a negative penalty (-1) when it hits the boundaries. Based on three different random seeds, we compare

¹<https://github.com/BillChan226/POAR-SRL-4-Robot>

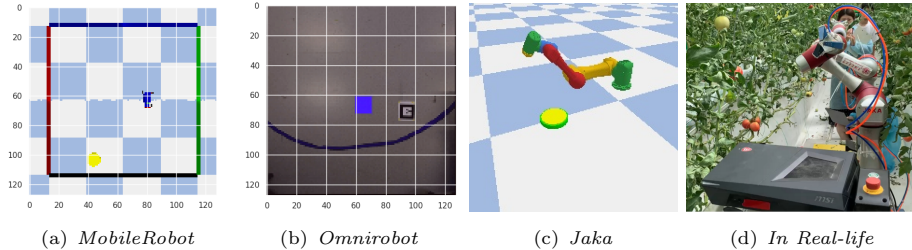


Fig. 3 Robotics environments that we select to perform experiments. *MobileRobot* aims to reach the yellow target with as few steps as possible. *Omnirobot* learns to circle the target by optimizing (5). *Jaka* is a 6-DOF mechanical robot manipulator.

POAR model with both split and combination optimization strategy to end-to-end PPO baseline and decoupling SRL with split strategy presented in [14].

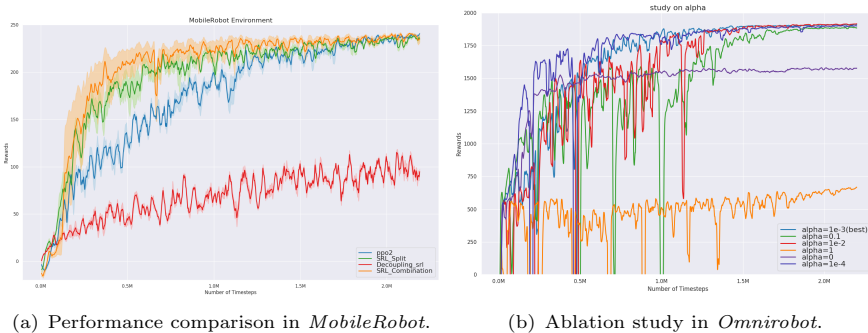


Fig. 4 (a): Results which compare POAR with original PPO and decoupling SRL method. (b): A study on trade off parameter α .

The improvement in performance of POAR model regardless of optimization strategy is illustrated in Fig. 4(a). The decoupling strategy is sensitive to splitting dimension due to the lack of a good metric to evaluate the SRL model, leading to unstable performance and over-fitting. On the contrary, since POAR can update to adapt to the task while RL agent explores to learn, it exhibits better convergent accuracy.

Omnirobot learns to circle the target by optimizing (5).

$$r_t = \lambda \times (1 - \lambda(\|z_t\| - R)^2) \times \|z_t - z_{t-k}\|_2^2 + \lambda^2 r_{t,bumped} \quad (5)$$

A main difference that distinguishes *Circling* from *Reaching* task is that the robot is encouraged to move away from the position after k steps. In *Omnirobot*, the robot learns not only how to circle the target but also how to avoid bumping into walls, namely to learn to follow a specific trajectory, which introduces more dynamical features. We carried out a set of thorough experiments to compare the SOTA RL algorithms on this typical environment.

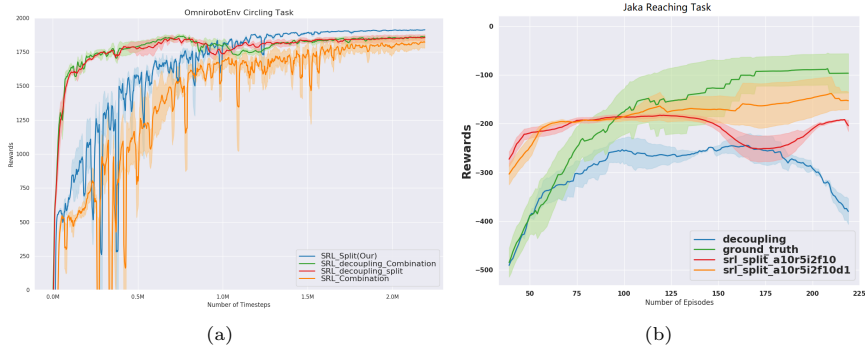


Fig. 6 (a): results in *Omnibot* which compare POAR with decoupling SRL strategy of split and combination weights attribution. (b): results in *Jaka* that demonstrates effectiveness of domain resemblance prior.

sample efficiency regardless of split or combination mode. However, they suffer from over-fitting over the state representation at the final stage of RL training, due to the lack of exploration. In addition, the abundant pre-sampling guarantees the convergence rate at the beginning of training for decoupling strategies, otherwise the bias as illustrated in Fig. 8(b) is difficult to overcome. Thus generally, POAR exhibits better sample efficiency, since the sampled data is leveraged to train both SRL and RL models.

We also compare performance on a more complex and dynamic environment *Jaka*, in which the robot tries to push the button on the ground. Results in Fig. 6(b) show that ground-truth coordinate is an informative enough state representation from which we can train an efficient agent. Thus it explains why the model with *domain resemblance* can outperform the one without, since a more structural perception of the environment space is built into the states.

4.2 Qualitative Analysis

In this subsection we provide an access for human-in-the-loop inspection, namely by monitoring the state graph iteration to diagnose current policy and SRL model. Firstly we show in Fig. 7 the reconstruction result of *MobileRobot* by introducing *domain resemblance* loss.

With such priors engaged, the interpretation of latent states is further enforced. Fig. 8(a) is a 2D projection, using PCA, of the state inferred by the SRL encoder, which we obtained via a policy at the beginning of training POAR (at episode 200). To better demonstrate and compare the rewards’ distribution, we project the learned states obtained by decoupling strategy to a 3D space, as shown in Fig. 8(b).

States learned with decoupling strategy (Fig. 8(b)) is sparser and have some holes at which the state estimator can’t offer the agent with sufficient information. Similarly, Fig. 9 presents the evolution of state graph with POAR in *Omnibot*.

At 1000th episode, we can observe the square boundary shape and reward distribution. At 3000th episode, we reach a policy that achieves reasonable rewards (1830

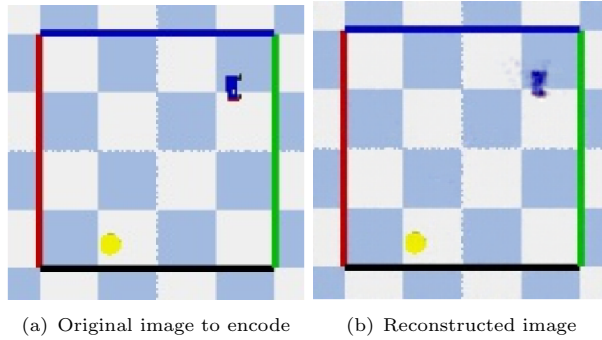


Fig. 7 Reconstruction result in *MobileRobot* by introducing domain resemblance prior.

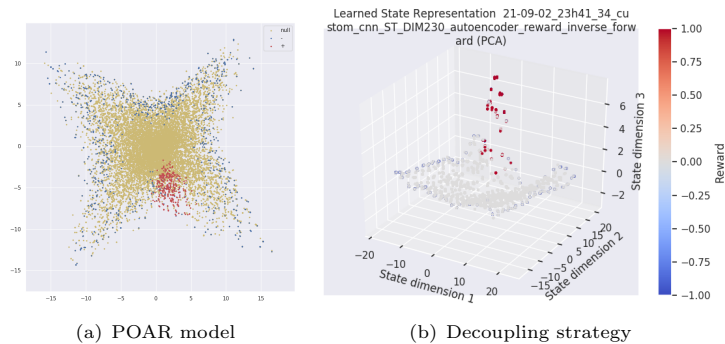


Fig. 8 Comparison between POAR and decoupling strategy of learned states in *MobileRobot*, respectively cast into 2D and 3D.

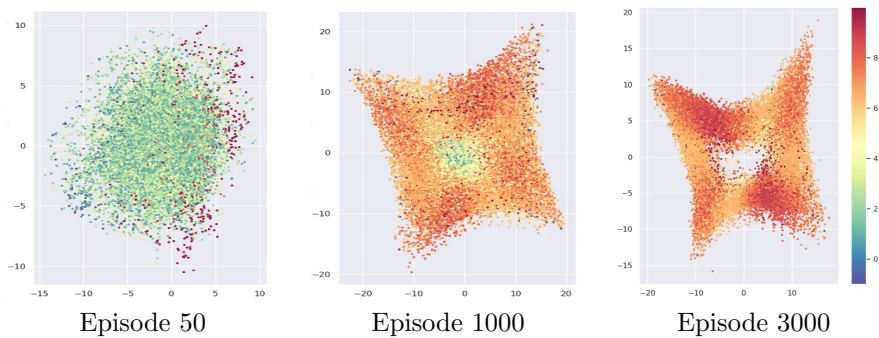


Fig. 9 The evolution of state graph in *Omnirobot* through the course of RL training with POAR model. Each episode consists of 250 time steps of interactions. We used split dimension with $dim_{reward} : 120$, $dim_{inverse} : 50$, $dim_{forward} : 50$. The weights assigned on such SRL model are: $w_{autoencoder} : 1$, $w_{reward} : 1$, $w_{inverse} : 5$, $w_{forward} : 5$.

scores within an episode). From the state at last checkpoint, we have a better understanding of the agent’s behavior: there is a specific direction that accumulates more rewards at four corners, which incites agent to circle around the center.

4.3 Ablation Study

As is shown in Fig. 4(b), we study how α , a hyperparameter that balances the trade off between RL and SRL loss, influences the training result. When $\alpha = 0.001$, the SRL model can best leverage the feedback from RL to improve itself, speeding up sample efficiency and improving stability.

Table 2 shows how the performance of POAR varies with respect to different weights attribution. We can denote that almost all weight choices outperform the PPO baseline, in terms of sample efficiency and final rewards.

Table 2 Policy regret normalized by PPO and rewards in *MobileRobot*.

w_a	w_r	w_i	w_f	Policy Regrets	Rewards (\pm std) ¹
1	0	0	0	1.128 (\pm 0.065)	
1	0	1	5	0.880 (\pm 0.019)	237.94 (\pm 4.06)
10	0	1	1	0.869 (\pm 0.140)	240.32 (\pm 1.11)
1	0	10	1	0.907 (\pm 0.049)	239.99 (\pm 2.69)
1	0	1	1	0.940 (\pm 0.105)	234.75 (\pm 3.22)
1	0	1	10	1.012 (\pm 0.076)	237.20 (\pm 0.65)
5	0	1	1	0.843 (\pm 0.073)	232.12 (\pm 6.12)
1	0	5	1	0.814 (\pm 0.067)	239.75 (\pm 3.18)
5	0	1	1	0.843 (\pm 0.073)	232.12 (\pm 6.12)
1	5	2	1	2.406 (\pm 0.042)	94.90 (\pm 1.04) ^d
1	5	2	1	0.684 (\pm 0.102)	236.21 (\pm 3.19) ^s
1	5	2	1	0.562 (\pm 0.228)	235.90 (\pm 4.32) ^c
PPO (Baseline)				1.000 (\pm 0.063)	234.242 (\pm 3.867)

¹ d denotes decoupling strategy; s denotes split mode; c denotes combination mode.

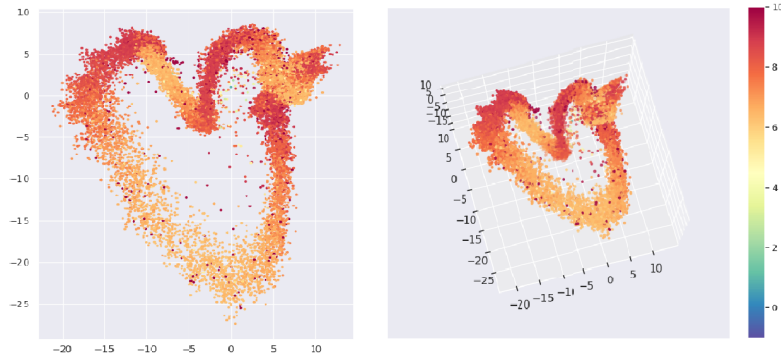


Fig. 10 State graph with different SRL weight attribution in *Omnibot*.

Fig. 10 shows inferred abstract state trained with SRL weights partition: $w_{reward} : 5$, $w_{inverse} : 2$, $w_{forward} : 1$ and with the same split dimension strategy as Fig. 9. The bias on reward model encourages state to separate points with different rewards in

higher dimension. Although it has a less physical meaning for robotic, yet, it has a better sample efficiency during training.

5 Conclusions

To conclude, we summarize the SOTA SRL sub-tasks in prior works and present a new framework to train RL agent together with the SRL model, as well as a *domain resemblance prior* to leverage expert demonstration. With such features incorporated, our framework can efficiently handle the tasks in high-dimensional robotic scenarios, and encourages the potential to train real-life robots from scratch. During training, POAR can provide real-time access to the current inferred states which helps to interpret RL with a real physical meaning, and we can thus monitor the course of training and diagnose the policy. In detail,

1. Our model integrates SRL into the training process of RL which allows SRL to adapt with RL. Learned in this way, the observation-state mapping can thus guarantee the high final rewards of RL, since over-fitting is overcome.
2. By reusing the interactions collected by RL for training SRL and leveraging expert demonstration to guide the agent, the cold-start problem is tackled and sample efficiency is substantially sped up.
3. Compared with the decoupling strategy, our model is more robust, almost all SRL models outperform the original PPO model in our setups. Hence, it is easier to tune the hyperparameter.

In terms of future work, we would like to thoroughly test our algorithm on other standard RL frameworks to explore the general performance of POAR. Inspired by this framework, we could also develop other RL architectures based on A3C, ACER and deepq algorithms to further boost the sample efficiency of reinforcement learning.

Appendix A Hyperparameters

Hyperparameter settings please refer to Table A1. All other hyperparameters that are not presented on the table are the same as the PPO2 implementation of *baselines* [43].

Hyperparameter	Value
lr (Optimizer 1)	5e-4
lr (Optimizer 2)	2.0e-4
α	0.001
β	20

Table A1 POAR hyperparameter settings

References

- [1] Schulman, J., Wolski, F., Dhariwal, P., Radford, A., Klimov, O.: Proximal policy optimization algorithms. arXiv preprint arXiv:1707.06347 (2017)

- [2] Kaiser, L., Babaeizadeh, M., Milos, P., Osinski, B., Campbell, R.H., Czechowski, K., Erhan, D., Finn, C., Kozakowski, P., Levine, S., et al.: Model-based reinforcement learning for atari. arXiv preprint arXiv:1903.00374 (2019)
- [3] Finn, C., Levine, S., Abbeel, P.: Guided cost learning: Deep inverse optimal control via policy optimization. In: International Conference on Machine Learning, pp. 49–58 (2016). PMLR
- [4] Chen, Z., Chen, B., Xie, S., Gong, L., Liu, C., Zhang, Z., Zhang, J.: Efficiently training on-policy actor-critic networks in robotic deep reinforcement learning with demonstration-like sampled exploration. In: 2021 3rd International Symposium on Robotics & Intelligent Manufacturing Technology (ISRIMT), pp. 292–298 (2021). IEEE
- [5] Garcia, J., Fernández, F.: A comprehensive survey on safe reinforcement learning. *Journal of Machine Learning Research* **16**(1), 1437–1480 (2015)
- [6] Chen, Z., Chen, B., He, T., Gong, L., Liu, C.: Progressive adaptive chance-constrained safeguards for reinforcement learning. arXiv preprint arXiv:2310.03379 (2023)
- [7] Bellman, R.: Dynamic programming. *Science* **153**(3731), 34–37 (1966)
- [8] Huang, W., Mordatch, I., Pathak, D.: One policy to control them all: Shared modular policies for agent-agnostic control. In: International Conference on Machine Learning, pp. 4455–4464 (2020). PMLR
- [9] Bengio, Y., Courville, A., Vincent, P.: Representation learning: A review and new perspectives. *IEEE transactions on pattern analysis and machine intelligence* **35**(8), 1798–1828 (2013)
- [10] Chen, T., Kornblith, S., Norouzi, M., Hinton, G.: A simple framework for contrastive learning of visual representations. In: International Conference on Machine Learning, pp. 1597–1607 (2020). PMLR
- [11] He, K., Fan, H., Wu, Y., Xie, S., Girshick, R.: Momentum contrast for unsupervised visual representation learning. In: Proceedings of the IEEE/CVF Conference on Computer Vision and Pattern Recognition, pp. 9729–9738 (2020)
- [12] Bachman, P., Hjelm, R.D., Buchwalter, W.: Learning representations by maximizing mutual information across views. *Advances in neural information processing systems* **32** (2019)
- [13] Schwarzer, M., Anand, A., Goel, R., Hjelm, R.D., Courville, A., Bachman, P.: Data-efficient reinforcement learning with self-predictive representations. arXiv preprint arXiv:2007.05929 (2020)

- [14] Raffin, A., Hill, A., Traoré, R., Lesort, T., Díaz-Rodríguez, N., Filliat, D.: Decoupling feature extraction from policy learning: assessing benefits of state representation learning in goal based robotics. arXiv preprint arXiv:1901.08651 (2019)
- [15] Zakka, K., Zeng, A., Florence, P., Tompson, J., Bohg, J., Dwibedi, D.: Xirl: Cross-embodiment inverse reinforcement learning. In: Conference on Robot Learning, pp. 537–546 (2022). PMLR
- [16] Liu, Y., Gupta, A., Abbeel, P., Levine, S.: Imitation from observation: Learning to imitate behaviors from raw video via context translation. In: 2018 IEEE International Conference on Robotics and Automation (ICRA), pp. 1118–1125 (2018). IEEE
- [17] Yu, T., Finn, C., Xie, A., Dasari, S., Zhang, T., Abbeel, P., Levine, S.: One-shot imitation from observing humans via domain-adaptive meta-learning. arXiv preprint arXiv:1802.01557 (2018)
- [18] Ding, M., Xu, Y., Chen, Z., Cox, D.D., Luo, P., Tenenbaum, J.B., Gan, C.: Embodied concept learner: Self-supervised learning of concepts and mapping through instruction following. In: Conference on Robot Learning, pp. 1743–1754 (2023). PMLR
- [19] Martín-Martín, R., Lee, M.A., Gardner, R., Savarese, S., Bohg, J., Garg, A.: Variable impedance control in end-effector space: An action space for reinforcement learning in contact-rich tasks. In: 2019 IEEE/RSJ International Conference on Intelligent Robots and Systems (IROS), pp. 1010–1017 (2019). IEEE
- [20] Shao, L., Ferreira, F., Jorda, M., Nambiar, V., Luo, J., Solowjow, E., Ojea, J.A., Khatib, O., Bohg, J.: Unigrasp: Learning a unified model to grasp with multi-fingered robotic hands. IEEE Robotics and Automation Letters **5**(2), 2286–2293 (2020)
- [21] Schwarzer, M., Rajkumar, N., Noukhovitch, M., Anand, A., Charlin, L., Hjelm, R.D., Bachman, P., Courville, A.C.: Pretraining representations for data-efficient reinforcement learning. Advances in Neural Information Processing Systems **34**, 12686–12699 (2021)
- [22] Grill, J.-B., Strub, F., Altché, F., Tallec, C., Richemond, P., Buchatskaya, E., Doersch, C., Avila Pires, B., Guo, Z., Gheshlaghi Azar, M., *et al.*: Bootstrap your own latent—a new approach to self-supervised learning. Advances in neural information processing systems **33**, 21271–21284 (2020)
- [23] Jonschkowski, R., Brock, O.: State representation learning in robotics: Using prior knowledge about physical interaction. In: Robotics: Science and Systems (2014)
- [24] Lange, S., Riedmiller, M., Voigtländer, A.: Autonomous reinforcement learning

- on raw visual input data in a real world application. In: The 2012 International Joint Conference on Neural Networks (IJCNN), pp. 1–8 (2012). IEEE
- [25] Jetchev, N., Lang, T., Toussaint, M.: Learning grounded relational symbols from continuous data for abstract reasoning. In: Proceedings of the 2013 ICRA Workshop on Autonomous Learning (2013)
- [26] Gelada, C., Kumar, S., Buckman, J., Nachum, O., Bellemare, M.G.: Deepmdp: Learning continuous latent space models for representation learning. In: International Conference on Machine Learning, pp. 2170–2179 (2019). PMLR
- [27] Guo, Z.D., Pires, B.A., Piot, B., Grill, J.-B., Alché, F., Munos, R., Azar, M.G.: Bootstrap latent-predictive representations for multitask reinforcement learning. In: International Conference on Machine Learning, pp. 3875–3886 (2020). PMLR
- [28] Finn, C., Tan, X.Y., Duan, Y., Darrell, T., Levine, S., Abbeel, P.: Learning visual feature spaces for robotic manipulation with deep spatial autoencoders. arXiv preprint arXiv:1509.06113 **25**, 2 (2015)
- [29] Lesort, T., Díaz-Rodríguez, N., Goudou, J.-F., Filliat, D.: State representation learning for control: An overview. *Neural Networks* **108**, 379–392 (2018)
- [30] Marler, R.T., Arora, J.S.: Survey of multi-objective optimization methods for engineering. *Structural and multidisciplinary optimization* **26**, 369–395 (2004)
- [31] Sun, T., Gong, L., Li, X., Xie, S., Chen, Z., Hu, Q., Filliat, D.: Robotdrlsim: A real time robot simulation platform for reinforcement learning and human interactive demonstration learning. In: *Journal of Physics: Conference Series*, vol. 1746, p. 012035 (2021). IOP Publishing
- [32] Argall, B.D., Chernova, S., Veloso, M., Browning, B.: A survey of robot learning from demonstration. *Robotics and autonomous systems* **57**(5), 469–483 (2009)
- [33] Gretton, A., Borgwardt, K.M., Rasch, M.J., Schölkopf, B., Smola, A.: A kernel two-sample test. *The Journal of Machine Learning Research* **13**(1), 723–773 (2012)
- [34] Munk, J., Kober, J., Babuška, R.: Learning state representation for deep actor-critic control. In: 2016 IEEE 55th Conference on Decision and Control (CDC), pp. 4667–4673 (2016). IEEE
- [35] Hjelm, R.D., Fedorov, A., Lavoie-Marchildon, S., Grewal, K., Bachman, P., Trischler, A., Bengio, Y.: Learning deep representations by mutual information estimation and maximization. arXiv preprint arXiv:1808.06670 (2018)
- [36] He, T., Zhang, Y., Ren, K., Liu, M., Wang, C., Zhang, W., Yang, Y., Li, D.: Reinforcement learning with automated auxiliary loss search. *Advances in Neural*

Information Processing Systems **35**, 1820–1834 (2022)

- [37] Kingma, D.P., Ba, J.: Adam: A method for stochastic optimization. arXiv preprint arXiv:1412.6980 (2014)
- [38] Xie, S., Gong, L., Chen, Z., Chen, B.: Simulation of real-time collision-free path planning method with deep policy network in human-robot interaction scenario. In: 2023 International Conference on Advanced Robotics and Mechatronics (ICARM), pp. 360–365 (2023). IEEE
- [39] Kober, J., Bagnell, J.A., Peters, J.: Reinforcement learning in robotics: A survey. *The International Journal of Robotics Research* **32**(11), 1238–1274 (2013)
- [40] Berlinet, A., Thomas-Agnan, C.: *Reproducing Kernel Hilbert Spaces in Probability and Statistics*. Springer, ??? (2011)
- [41] Todorov, E., Erez, T., Tassa, Y.: Mujoco: A physics engine for model-based control. In: 2012 IEEE/RSJ International Conference on Intelligent Robots and Systems, pp. 5026–5033 (2012). IEEE
- [42] Graves, A., Graves, A.: Long short-term memory. *Supervised sequence labelling with recurrent neural networks*, 37–45 (2012)
- [43] Dhariwal, P., Hesse, C., Klimov, O., Nichol, A., Plappert, M., Radford, A., Schulman, J., Sidor, S., Wu, Y., Zhokhov, P.: Openai baselines (2017)

Declarations

1.1 Funding

This work was supported by Shanghai Agriculture Applied Technology Development Program, China (Grant No.C2019-2-2) and National Key Research and Development Program “Robotic Systems for agriculture(RS-Agri)” (2019YFE0125200).

1.2 Competing Interests

The authors have no relevant financial or non-financial interests to disclose.

1.3 Author Contributions

Zhaorun Chen: Conceptualization, Investigation, Formal analysis, Writing (original draft). **Liang Gong, Binhao Chen:** Investigation, Formal analysis, Writing (original draft). **Siqi Fan, Yuan Tan:** Investigation, Formal analysis. **Te Sun, David Filliat, Natalia Díaz-Rodríguez:** Conceptualization, Writing (review & editing), Supervision. **Chengliang Liu:** Project administration, Funding acquisition.

1.4 Ethics approval

Not Applicable.

1.5 Consent to participate

Not Applicable.

1.6 Consent to publish

Not Applicable.